Employment of Interpolated DFT-based PMU Algorithms in Three-Phase Systems

Roberto Ferrero*, Paolo Attilio Pegoraro**, Sergio Toscani***
**Department of Electrical Engineering & Electronics, University of Liverpool, Liverpool, United Kingdom
roberto.ferrero@liverpool.ac.uk
*Department of Electric and Electronic Engineering, University of Cagliari, Cagliari, Italy
paolo.pegoraro@diee.unica.it
***Dipartimento di Elettronica, Informazione e Bioingegneria, Politecnico di Milano, Milano, Italy
sergio.toscani@polimi.it

***Abstract*—Phasor measurement units (PMUs) are the key measurement devices of modern power networks monitoring systems. The high accuracy and fast reporting rates required for PMU implementations ask for improvements in both hardware and software solutions. Depending on the characteristics of the monitored voltages and currents, the accuracy of PMU algorithms may represent the main contribution to the overall measurement performance. For this reason, research is ongoing in the field of signal processing techniques for phasor and frequency estimation. In this context, Interpolated Discrete Fourier Transform (IpDFT) is one of the most interesting techniques, mainly because it allows accurate measurements under off-nominal frequency conditions while preserving simplicity and computational efficiency. In this paper, the applicability of IpDFT to three-phase signals that are typical of power networks is discussed. Then, it is proposed to combine the advantages of IpDFT with those of the Space Vector approach for positive sequence synchrophasor and frequency measurements.**

Keywords— Phasor Measurement Units (PMU); Voltage Measurement; Current Measurement; Frequency; Total Vector Error (TVE).

I. INTRODUCTION

Phasor measurement units (PMUs) are becoming the most interesting instrument in the monitoring of power networks. PMUs provide a coordinated and synchronized current and voltage phasor monitoring across different nodes of the network. Their role is particularly important in Wide Area Monitoring Systems (WAMS) of power transmission systems, which are rapidly growing both in pervasivity and reliability. Nevertheless, the interest for the use of PMU and PMU-enabled devices is widespread, in particular when looking towards the future scenarios of distribution networks and the smart grids.

Since PMU is the sensing unit of the monitoring infrastructure, its performance plays a key role also on the upper layers of management and control applications that are expected to catch on in an automation perspective. For this reason, the focus is nowadays moved on the design of the instruments in all their aspects, from synchronization to acquisition including the computational issues a PMU has to tackle.

In particular, in the last years, great attention has been paid to PMU algorithms, because, when considering input signals that deviate from nominal frequency and purely sinusoidal steady-state conditions, the adopted phasor measurement technique can be the main source of measurement error. In the literature, several signal processing methods have been proposed and tested in the context of synchrophasor measurements; different approaches have been explored, aiming at different targets, according to the class of the input signals. A general overview of the recent contributions can be found, for example, in [1].

One of the most popular techniques for implementing PMU measurement algorithms is certainly the Interpolated Discrete Fourier Transform (IpDFT) along with its variants. IpDFT comes from the spectral analysis world, thus is perfectly suited when spectral line measurement is concerned. For this reason, the employment of IpDFT has been recently investigated for PMU applications, where the characteristic parameters (amplitude, phase angle, and frequency) of the fundamental component of voltages or currents have to be estimated.

In [2], the accuracy of the multicycle IpDFT is assessed, through numerical simulation, by considering the test signals given by the standard IEEE C37.118.1 [3] and the corresponding limits in terms of maximum total vector error (TVE). On the other hand, in [4] a PMU prototype based on an enhanced version of the IpDFT is proposed. These researches highlight the applicability of the IpDFT approach in the context of PMU.

Even though there is a rich literature about IpDFT, its extensions, configurations and implementations, less attention is paid to its peculiarities when applied to three-phase quantities. In many important cases, frequency and positive sequence synchrophasor estimations are required. Such applications include monitoring and state estimation of high voltage power systems, but often the balanced assumption holds also for medium voltage grids during regular operation. Under this hypothesis, Space Vector (SV) based estimation methods [9], [10] have shown considerable advantages. For

this reason, the present paper proposes to combine the SV approach with the frequency-domain interpolation typical of IpDFT-based techniques. The aim is to investigate the performance of the resulting algorithms that appear promising for PMUs installed in three-phase systems.

II. Conventional Interpolated DFT algorithm

Let us consider a real-valued sinusoidal signal x whose time-domain expression is given by:

$$x(t) = \sqrt{2} X_1 \cos(\omega_1 t + \varphi_1) \tag{1}$$

being $\omega_1 \geq 0$ the angular frequency and $X_1 \geq 0$ the rms amplitude. This signal may represent a voltage or current waveform in an ac power system, characterized by the rated frequency f_0 and the rated angular frequency ω_0. Its spectrum $\bar{X}(j\omega)$ is obtained analytically by applying the generalized Fourier Transform, thus resulting:

$$\bar{X}(j\omega) = \frac{\sqrt{2}X_1}{2}\left[e^{j\varphi_1}\delta(j\omega_1 - j\omega) + e^{-j\varphi_1}\delta(-j\omega_1 - j\omega)\right] \tag{2}$$

where δ denotes the Dirac delta distribution. It is clear that the Fourier transform contains information about the synchrophasor and frequency characterizing the signal. However, this computation is not feasible from a practical point of view: the waveform, assumed to be purely sinusoidal and stationary, has to be observed over an unlimited time interval.

Practical frequency-domain synchrophasor measurement algorithms require to sample the time-domain signal with a proper interval T_s, corresponding to the rate f_s which is usually a multiple of the rated frequency:

$$f_s = M f_0 \tag{3}$$

The acquired signal is processed considering the N samples. The finite observation time result in a limited latency and in the capability to track slow changes of the sinewave parameters. Typically $N=KM$, with K positive integer, so that an integer number of periods at the rated frequency is processed. A suitable weighting window is applied to the acquired data in order to reduce spectral leakage effects that appears when $\omega_1 \neq \omega_0$; let us call $w(m)$ (m ranging from 0 to N-1) their real-valued weighting coefficients. Considering the time instant nT_s, the windowed signal results:

$$x_w(nT_s, m) = \sqrt{2} X_1 w(m) \cos(\omega_1 (n + m - N + 1) T_s + \varphi_1) \tag{4}$$

The Discrete Fourier Transform (DFT) of the windowed signal $\bar{X}_w(nT_s, jk\omega_b)$ is computed using the well-known algorithm, where ω_b is the frequency resolution:

$$\omega_b = \frac{\omega_0}{K} \tag{5}$$

$\bar{X}_w(nT_s, jk\omega_b)$ can be also expressed as the convolution between the Fourier transform of the continuous time signal x and the discrete time Fourier Transform of the window $\bar{W}(j\omega)$:

$$\bar{X}_w(nT_s, jk\omega_b) = \frac{1}{2\pi}\left[\bar{X}(j\omega) e^{j\omega(n-N+1)T_s} * \bar{W}(j\omega)\right](jk\omega_b) \tag{6}$$

where the exponential term, corresponding to a time shift, takes into account the slip between window and signal. Substituting the analytic expression of $\bar{X}(j\omega)$:

$$\bar{X}_w(nT_s, jk\omega_b) = \frac{\sqrt{2}X_1}{2}\left[\bar{W}(jk\omega_b - j\omega_1) e^{j\left[\omega_1 (n-N+1)T_s + \varphi_1\right]} + \right. \\ \left. + \bar{W}(jk\omega_b + j\omega_1) e^{-j\left[\omega_1 (n-N+1)T_s + \varphi_1\right]}\right] \tag{7}$$

In general, each DFT term depends on both the two spectral lines of the input signal. Let us consider the highest DFT component, having positive frequency $\tilde{k}\omega_b$. Assuming that the spectral interference is negligible thanks to the window:

$$\bar{X}_w(nT_s, j\tilde{k}\omega_b) \cong \frac{\sqrt{2}X_1}{2}\bar{W}(-j\varepsilon\omega_b) e^{j\left[\omega_1 (n-N+1)T_s + \varphi_1\right]} \tag{8}$$

Having defined:

$$\varepsilon = \frac{\omega_1}{\omega_b} - \tilde{k} \tag{9}$$

whose absolute value is below 0.5. The magnitude of $\bar{X}_w(nT_s, j\tilde{k}\omega_b)$ is proportional to that of the positive spectral line in the signal, but it is affected by scalloping loss due to non-coherent sampling. This effect can be compensated by using frequency-domain interpolation. The simplest two-point algorithm [5], known as Interpolated DFT (IpDFT), requires applying a window whose main lobe is at least $2L$ bins wide, with $L \geq 2$. Assuming $K \geq L$ and considering (7) there are at least three DFT terms produced by the positive-frequency spectral line of the signal falling below the main lobe of the window during the convolution. The highest has angular frequency $\tilde{k}\omega_b$, while the second highest $\tilde{k}_\gamma \omega_b$, that can be equal to $(\tilde{k}+1)\omega_b$ or $(\tilde{k}-1)\omega_b$. Neglecting long-range leakage phenomena, the ratio γ between the magnitudes of the two highest DFT components results:

$$\gamma = \frac{\max\left(W(j(1+\varepsilon)\omega_b), W(j(1-\varepsilon)\omega_b)\right)}{W(-j\varepsilon\omega_b)} \tag{10}$$

Reminding that the window magnitude response W is an even function, γ just depends on the window shape and on the absolute value of ε. Therefore, by computing this ratio and knowing the shape of the window $|\varepsilon|$ is obtained, and hence also the signal frequency:

$$\tilde{f}_1 = \left(\tilde{k} + \mathrm{sgn}\left(\tilde{k}_\gamma - \tilde{k}\right)|\varepsilon|\right)\frac{\omega_b}{2\pi} \tag{11}$$

Analytic expressions [6] exists for Rife-Vincent class I windows [7], otherwise lookup tables can be employed [8]. Short-range leakage effects can be compensated, while the sinewave rms amplitude and phase are estimated as:

$$\tilde{X}_1 = \sqrt{2}\frac{X_w\left(nT_s, jk\tilde{\omega}_b\right)}{W\left(-j\varepsilon\omega_b\right)} \qquad (12)$$
$$\tilde{\varphi}_1 = \angle\bar{X}_w\left(nT_s, jk\tilde{\omega}_b\right)$$

Finally, group and phase delays due to the window have to be removed in order to obtain synchrophasor and frequency estimations. The method does not directly provide a rate of change of frequency (ROCOF) estimation. However, it can be obtained by numerically differentiating the frequency measurement.

III. Space-Vector Interpolated DFT algorithm

Interpolated DFT can be usefully employed to evaluate the synchrophasor and frequency of ac power systems signals [2]. Electrical quantities are inherently three-phase, so the aforementioned algorithm has to be applied three times, one for each phase. Furthermore, many applications require the positive sequence synchrophasor, which is obtained by applying the Fortescue transformation to the three single-phase synchrophasors.

As from the synchrophasor standard, frequency is unique for each three-phase quantity; on the contrary, when the IpDFT algorithm is employed, frequency estimations for each phase are provided. Sometimes, the three single-phase frequency measurements are averaged in order to derive a unique value. It becomes clear that this approach is somewhat questionable. Reference methods proposed by the standard [3] estimate frequency as its rated value plus the rotational speed of the positive sequence synchrophasor divided by 2π. In this way, angular frequency has a strong physical meaning: it corresponds to the angular speed of the air-gap field produced by a three-phase symmetrical current or voltage, defined by the positive sequence synchrophasor and applied to a two-pole, three phase balanced stator winding.

Furthermore, it should be noticed that the main assumption behind IpDFT algorithms is that long-range leakage has to be negligible, hence that the effect of the negative frequency term of the input sinewave on the amplitudes of the two largest positive-frequency DFT components is not significant, so (10) can be written and inverted. Unfortunately, it is not always true when low-latency synchrophasor and frequency estimation is required, such as in P-class PMUs. In this case, a short-length window must be employed, but it is not able to suppress a disturbance (negative frequency term) having the same amplitude as the useful component.

For this reason, frequency domain interpolation algorithms aimed at reducing the effect of the so-called negative frequency image have been proposed [4]. The drawback is that complexity increases together with the computational burden.

When the target is estimating the positive sequence synchrophasor, Space Vector (SV) based methods [9], [10] can be employed. A SV approach can be combined with frequency domain interpolation, thus leading to considerable simplifications. For the purpose, let us consider a three-phase balanced signal:

$$\mathbf{x}_{abc}(t) = \begin{vmatrix} x_a(t) \\ x_b(t) \\ x_c(t) \end{vmatrix} = \sqrt{2}X_1 \begin{vmatrix} \cos\left(\omega_1 t + \varphi_1\right) \\ \cos\left(\omega_1 t + \varphi_1 - \frac{2\pi}{3}\right) \\ \cos\left(\omega_1 t + \varphi_1 + \frac{2\pi}{3}\right) \end{vmatrix} \qquad (13)$$

The corresponding positive sequence phasor is:

$$\bar{X}_+ = X_+ e^{j\varphi_+} = \sqrt{3}X_1 e^{j\varphi_1} \qquad (14)$$

As usual, the three time-domain signals are acquired with proper sampling rate f_s. After that, the SV transformation on a stationary reference frame is applied. The SV $\bar{x}_{SV}$ is obtained as:

$$\bar{x}_{SV}\left(nT_s\right) = \sqrt{\frac{2}{3}}\begin{vmatrix} 1 & \bar{\alpha} & \bar{\alpha}^2 \end{vmatrix}\mathbf{x}_{abc}\left(nT_s\right) \qquad (15)$$

Where $\bar{\alpha} = e^{j2\pi/3}$. Performing simple computations leads to:

$$\bar{x}_{SV}\left(nT_s\right) = \bar{X}_+ e^{j\omega_1 nT_s} \qquad (16)$$

In this case, the SV contains a unique term rotating in the complex plane with an angular speed ω_1. Its amplitude and initial phase are given by the positive sequence phasor. Possibly a counter-rotating term may be present because of the (slight) unbalance in the three phase quantities, but its magnitude is at most a few percentage points of X_+. A suitable window has to be applied to the space vector and its DFT can be computed. Frequency domain interpolation can be applied as explained in the previous section, but now long-range leakage artifacts are inherently negligible. Finally, positive sequence synchrophasor and frequency are obtained straightforwardly, requiring about one third of the computational burden with respect to the usual IpDFT.

IV. Simulation Results

The algorithms are tested by means of numerical simulations under MATLAB environment using a 1 kHz sampling rate. The test signals are generated according to the standard IEEE C37.118.1-2011 [3] and its amendment IEEE C37.118.1a-2014 [11]. Three-phase balanced signals for 50 Hz systems are used, as indicated in the standards, and the focus is firstly on off-nominal frequency conditions in the range [45 Hz, 55 Hz], as for M-class compliance tests.

Fig. 1 summarizes the synchrophasor measurement accuracy, in terms of TVE %, achieved by different methods under off-nominal frequency conditions. The SV-based IpDFT (SV-IpDFT) directly returns the positive sequence synchrophasor, while, for the conventional IpDFT algorithm, it has been obtained by applying the Fortescue transformation to

the three phase synchrophasor measurements; in both cases, 2-cycle Hann windows have been used. In addition, the maximum TVE % achieved by the IpDFT in estimating the synchrophasor of each phase is also reported. It is interesting to notice that in this case quite large errors under off-nominal frequency conditions appear, but they are almost cancelled in positive sequence estimations. The errors in single-phase measurements are due to the image component that directly affects synchrophasor and frequency estimations, and, as a consequence, also scalloping loss compensation. Using the SV approach, the negative frequency term is only due to the negative sequence component and thus it does not appear under balanced conditions. As for the IpDFT, when the Fortescue transformation is applied to obtain positive sequence from single-phase phasors, a compensation between errors appearing in the single phases takes place, but, as it can be argued from the zoom box inset of Fig. 1, a full cancellation is not achieved, because the transformation only acts as a complex-coefficient, three-point averaging filter.

Similar considerations hold for the frequency estimation (see Fig. 2) that is affected by spectral leakage effects due to the image component. In this case, it is important to highlight how the three-phase approach allows limiting FE, while the SV transformation permits a single frequency computation with higher accuracy and lower computational effort.

Simulations have been performed in order to analyze the impact of window length: 2, 4 and 6 cycles Hann windows have been considered. Table I summarizes the results in terms of maximum percent TVEs and FEs for the estimations. As expected, the effect of long-range leakage decreases considerably with longer windows that result in higher accuracy.

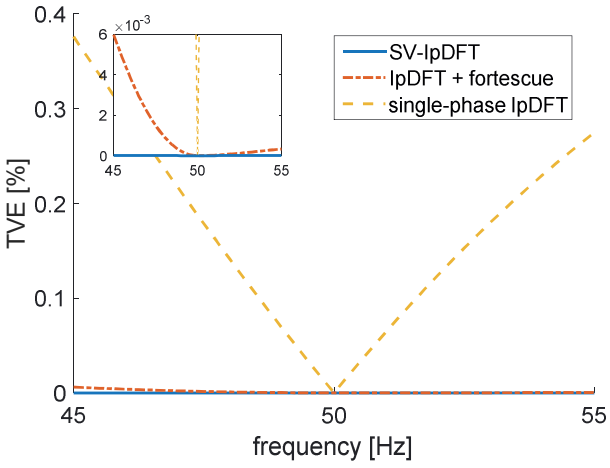

Fig. 1 Maximum TVE % for synchrophasor estimation, single- and three-phase signals.

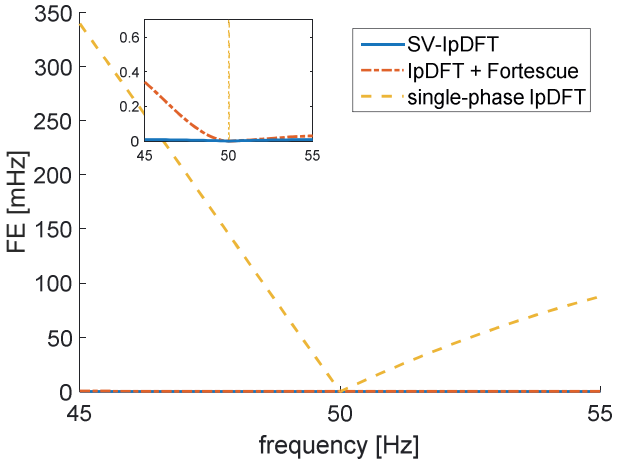

Fig. 2 Maximum frequency error, single- and three-phase signals

TABLE I. MAXIMUM TVE % AND FE, HANN WINDOWS OF DIFFERENT LENGTHS

Method	Window Length [number of nominal cycles]					
	2		4		6	
	TVE [%]	FE [mHz]	TVE [%]	FE [mHz]	TVE [%]	FE [mHz]
SV-IpDFT	9E-6	0.009	8E-7	0.3E-3	2E-7	4E-5
IpDFT+ Fortescue	0.003	0.342	8E-5	1.2E-3	5E-6	8E-5
Single-phase IpDFT	0.376	339.542	0.078	20.026	0.032	3.599

The results of the tests in presence of harmonics (as defined by [3]) are not reported since, thanks to the zeros of the Hann window in the frequency domain, disturbances having frequencies that are multiples of the nominal one are completely rejected.

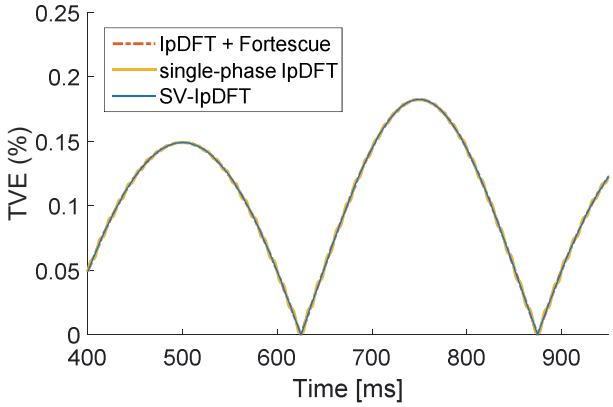

Fig. 3 TVE %, 2 Hz amplitude modulation.

As an example of dynamic test, Fig. 3 and Fig. 4 show the behavior of the previously discussed IpDFT algorithms employing a 4-cycle Hann window in presence of 2 Hz amplitude modulation. In this case, the underlying model (8) of the IpDFT algorithm no longer holds because of the multifrequency spectrum of the signal. Nevertheless, as for the synchrophasor estimation, the TVEs are rather low, but small oscillations due to the negative frequency component can be noticed when the single-phase algorithm is considered. Although errors are quite small also in this case, jumps appear in the frequency estimations. These jumps may lead to severe problems if the ROCOF is obtained by differentiating the measured frequency. In terms of maximum frequency error, the SV approach behaves almost like the single-phase DFT, because the model mismatch is prevailing at nominal frequency. However, the rate of the jumps is considerably lower when the SV approach is employed. If the frequency is computed by averaging the frequency estimations obtained by applying the conventional IpDFT to the three phases, it should be noticed that the frequency error becomes exactly one third. This happens because the jumps in the estimated frequencies of the three phases occur at different time instants.

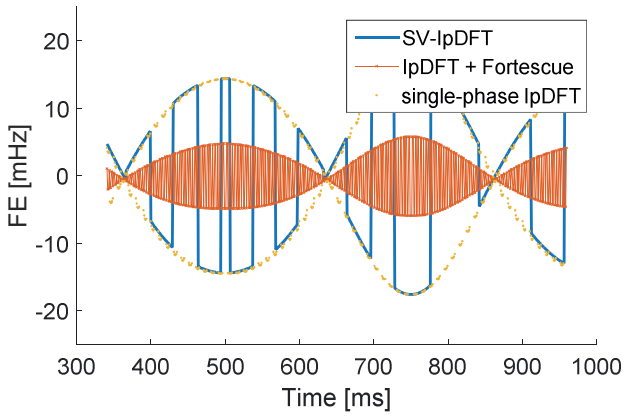

Fig. 4 Frequency error waveforms, 2 Hz amplitude modulation.

Finally, the frequency ramp test suggested by [11] has been performed by considering a 45 Hz to 55 Hz range and constant ROCOF equal to 1 Hz/s. Results obtained for a 4-cycle Hann window are reported in Table II. When looking at FEs, values are similar to those obtained in the off-nominal frequency test. On the contrary, TVEs are significantly higher because of the mismatch between the signal and the underlying model of the IpDFT approach.

TABLE II. MAXIMUM TVE % AND FE, 4-CYCLE HANN WINDOW

Performance index	**Method**		
	SV-IpDFT	**IpDFT+ Fortescue**	**Single-phase IpDFT**
TVE [%]	0.066	0.066	0.132
FE [mHz]	5.9E-3	8.2E-3	19.829

V. CONCLUSION

The IpDFT is a widespread tool for estimating amplitude, phase and frequency of a sinusoidal signal. It is particularly interesting because it combines steady-state accuracy with computational efficiency. For this reason, it represents an established technique for PMU implementation.

In this paper, the application of IpDFT to three-phase systems is discussed: significant differences with single-phase estimations are highlighted. In particular, it is shown how the SV approach and IpDFT complement each other very well. The negative frequency infiltration is one of the well-known weaknesses of classical IpDFT and the SV dramatically reduces its impact, since the disturbing component amplitude is reduced from the main component amplitude to that of the negative sequence component.

Therefore, it is clear that the peculiarities of three-phase systems can be exploited to improve the accuracy of other PMU measurement techniques, thus opening further research perspectives.

REFERENCES

[1] C. Muscas and P. A. Pegoraro, “Algorithms for synchrophasors, frequency, and rocof,” in Phasor Measurement Units and Wide Area Monitoring Systems, 1st ed., A. Monti, C. Muscas, and F. Ponci, Eds. Elsevier, Academic Press, 2016, ch. 3, pp. 21–51.

[2] D. Belega and D. Petri, "Accuracy Analysis of the Multicycle Synchrophasor Estimator Provided by the Interpolated DFT Algorithm," *IEEE Trans. Instrum. Meas.*, vol. 62, no. 5, pp. 942-953, May 2013.

[3] *IEEE Standard for Synchrophasor Measurements for Power Systems*, IEEE Std C37.118.1-2011.

[4] P. Romano and M. Paolone, "Enhanced Interpolated-DFT for Synchrophasor Estimation in FPGAs: Theory, Implementation, and Validation of a PMU Prototype," *IEEE Trans. Instrum. Meas.*, vol. 63, no. 12, pp. 2824-2836, Dec. 2014.

[5] V. K. Jain, W. L. Collins and D. C. Davis, "High-accuracy analog measurements via interpolated FFT," *IEEE Trans. Instrum. Meas.*, vol. IM-28, pp. 11 3-122, June 1979.

[6] J. Schoukens, R. Pintelon and H. Van Hamme, “The interpolated fast Fourier transform: A comparative study,” *IEEE Trans. Instrum. Meas.*, vol. 41, no. 2, pp. 226–232, Apr. 1992.

[7] D. C. Rife and G. A. Vincent, “Use of the discrete Fourier transform in the measurement of frequencies and levels of tones,” *Bell Syst. Tech. J.*, vol. 49, pp. 197–228, 1970.

[8] A. Ferrero, S. Salicone and S. Toscani, "A Fast, Simplified Frequency-Domain Interpolation Method for the Evaluation of the Frequency and Amplitude of Spectral Components," *IEEE Trans. on Instrum. and Meas.*, vol. 60, no. 5, pp. 1579-1587, May 2011.

[9] S. Toscani and C. Muscas, “A space vector based approach for synchrophasor measurement,” in *Proc. Int. Instrumentation and Measurement Technology Conf.*, May 2014, pp. 257–261.

[10] S. Toscani, C. Muscas and P. A. Pegoraro, “Design and performance prediction of space vector based PMU algorithms,” *IEEE Trans. on Instrum. Meas.*, vol. 66, pp. 394-404, March 2017.

[11] *IEEE Standard for Synchrophasor Measurements for Power Systems* -- Amendment 1: Modification of Selected Performance Requirements, IEEE Std C37.118.1a-2014 (Amendment to IEEE Std C37.118.1-2011).